Cytotechnology **32:** 97–107, 2000.

Metabolic-flux analysis of hybridoma cells under oxidative and reductive stress using mass balances

Hendrik P.J. Bonarius[1,*], José H.M. Houtman[1,3], Georg Schmid[1], Cornelis D. de Gooijer[2] & Johannes Tramper[2]

[1] *Department PRF-Biotechnology, Hoffman-La Roche Ltd., Bldg. 66/112, CH-4002 Basel, Switzerland;* [2] *Department of Food Science, Food and Bioengineering Group, Wageningen Agricultural University, P.O. Box 8129, 6700 EV Wageningen, The Netherlands;* [3] *present address: Bio R&D, Fort Dodge Animal Health Holland, Weesp, The Netherlands*

(Author for correspondence, present address: Department of Cell Biology, Novo Nordisk Ltd., HAB 1.094, Niels Steensenvej 1, 2820 Gentofte, Denmark)*

Received 29 January 1999; accepted 30 August 1999)

Key words: artificial electron acceptor, dehydrogenases, mammalian-cell culture, metabolic flux, oxygen limitation

Abstract

Hybridoma cells were grown at steady state under both reductive and oxidative stress and the intracellular fluxes were determined by mass-balancing techniques. By decreasing the dissolved oxygen pressure (pO_2) in the bioreactor, the reduced form of nicotinamide adenine nucleotide (NADH) was enhanced relative to the oxidized form (NAD^+). Oxidative stress, as a result of which the $NAP(P)^+$/NAD(P)H-ratio increases, was generated by both the enhancement of the pO_2 to 100% air saturation and by the addition of the artificial electron acceptor phenazine methosulphate (PMS) to the culture medium. It was found that fluxes of dehydrogenase reactions by which NAD(P)H is produced decreased under hypoxic conditions. For example, the degradation rates of arginine, isoleucine, lysine and the glutamate dehydrogenase flux were significantly lower at oxygen limitation, and increased at higher pO_2 levels and when PMS was added to the culture medium. In contrast, the proline synthesis reaction, which requires NADPH, decreased under PMS stress. The flux of the NADH-requiring lactate dehydrogenase reaction also strongly decreased from 19 to 3,4 pmol/cell/day, under oxygen limitation and under PMS stress, respectively. The data show that metabolic-flux balancing can be used to determine how mammalian respond to oxidative and reduction stress.

Nomenclature

Metabolites: AAA, Acetoacetate; ACoA, acetyl-CoA; AKG, alpha-ketoglutarate; CHOL, cholesterol; CIT, citrate; E4P, erythrose-4-phosphate; FA, fatty acids; FAD, flavin adenine dinucleotide, FAD^+, oxidized form of FAD; $FADH_2$, reduced form of FAD; GAP, glyceraldehyde 3-phosphate; Glc, glucose; G6P, glucose-6-phosphate; G3P, 3-Phosphoglycerate; Lac, lactate; MAB, monoclonal antibody; MAL, malate; NAD(P), nicotinamide adenine nucleotide (phosphate); $NAD(P)^+$, oxidized form of NAD(P); NAD(P)H reduced form of NAD(P); OAA, oxaloactetate; PEP, phosphoenolpyruvate; PL, phospholipids; PYR, pyruvate; R5P, ribose-5-phosphate; Ru5P, ribulose-5-phosphate; S7P, sedoheptulose-7-phosphate; SuCoA, Succinyl coenzyme A; THF, tetrahydrofolate; TC, total carbohydrates; TP, total protein; X5P, xylulose-5-phosphate.

Abbreviations: CER, carbon dioxide evolution rate; TCA, tricarboxylic acid; OUR, oxygen uptake rate; PMS, Phenazine methosulphate; PPS, pentose phosphate shunt; RQ respiration quotient.

Introduction

The intracellular fluxes of microorganisms, animal cells or tissue culture can be determined if the extracellular production and uptake rates of the relevant metabolities and the reaction stoichiometry of fluxes are known (Vallino and Stephanopoulos, 1989). This methodology, referred to as 'metabolic-flux balancing' (Varma and Palsson, 1994) has been proposed as an alternative (or supplement) to isotopic-racer studies for metabolic-flux analysis.

Although mass-balancing can be used to determine a large fraction of fluxes in metabolic networks, a number of pathways cannot be quantified due to the fact that the required set of linear mass-balance equations is underdetermined (Vallino and Stephanopoulos, 1989; Bonarius et al., 1997). This accounts in particular for linearly dependent reactions associated with cyclic metabolic pathways. Fluxes in cyclic pathways such as the CA cycle, the pentose-phosphate shunt, or the malate shunt cannot be determined by measurement of the extracellular production and uptake rates of the relevant metabolites alone. Additional constraints, usually obtained by isotopic-trcaer experiments are required to solve underdetermined metabolic networks, and thus to quantify fluxes in cyclic pathways.

Yet, mass-balancing techniques have been used for many applications in mammalian-cell culture, such as physiology studies, rational medium design, and analysis of bottle-necks in waste metabolism. For example, it was shown by linear-optimization techniques how fat synthesis constraints other metabolic pathways in adipose tissue (Fell and Small, 1986), and that the growth rate of hybridoma cells is neither limited by the ATP-maintenance demand nor by the antibody production rate (Savinell and Palsson, 1992). Sharfstein and co-workers (1994) used mass balances to complement ^{13}C-NMR data from hybridoma cells cultured in hollow-fiber bioreactors. It was found that both at low and high glutamine concentrations a significant fraction of amino acids entered the TCA-cycle at acetyl-CoA (f.e., isoleucine, leucine, lysine) and succinyl-CoA (isoleucine, methionine, and valine). At low glutamine concentrations, only 24% of the amino acids entered the TCA-cycle via α-ketoglutarate (which is mainly glutamine). These data show that it is important not only to balance glutamine, but also other amino acids for optimal process conditions. This was successfully done by Xie and Wang (1994, 1996). Based on stoichiometric analysis and mass-balancing techniques they designed a process-control strategy to meet the requirements for energy and growth of fed-batch-cultured hybridoma cells. The production of lactate, ammonia and amino acids was reduced, while avoiding substrate limitation for biomass synthesis and energy. This led to an efficient cell culture process with the final antibody titers as high as 2.4 g/L.

Metabolic-flux balancing has been used to analyze changes in intracellular flux distributions as a function of different culture conditions or differences in genotypes. Zupke and coworkers (1995) demontrated using metabolic balances that the pyruvate-dehydrogenase flux decreases and the glutamate-dehydrogenase flux reverses in hybridoma cells cultured at low oxygen tension. The effect of tissue hydrolysates, commonly used as efficient carbon and nitrogen sources in cell-culture media, has been investigated by similar techniques in a search for optimal intracellular flux distributions (Bonarius et al., 1996; Nyberg et al., 1999). Recently, it was shown by flux-balancing techniques that hybridoma cells cultured in a chemastat utilize pyruvate carbon more efficiently at lower dilution rates (Follstad et al., 1999). We showed that under ammonia stress hybridoma cells increase their glutamate-dehydrogenase flux, thus identifying glutamate dehydrogenase as a potential site for engineering ammonia-tolerant mammalian cells (Bonarius et al., 1998a).

These results suggest that flux-balancing techniques can be used to determine the intracellular effects of mammalian cells to stress and toxic agents only by the measurement of the uptake and production rates of relevant metabolites. Here, we apply mass-balancing techniques to determine intracellular fluxes of continuously cultured hybridoma cells under different types of stress. Hybridoma cells are cultured under conditions that affect the availability of the electron carriers NAD and NADP. It is shown for those metabolic fluxes that can be determined by mass-balancing techniques alone (that is, by measuring the biomass and the relevant metabolites) that NAD(P)H-producing reactions are activated under oxidative stress, and that the opposite occurs under reductive stress.

Materials and methods

Culture conditions and analyses

A detailed description of the various experimental procedures was published before (Bonarius et al., 1996). Briefly, hybridoma cells were cultured in a lab-scale bioreactor (Biostat MD, Braun, Melsungen, D) in a continuous mode at a dilution rate of 0.7 d^{-1}. A mixture of Dulbecco's Ham's F12 an Iscove's powdered medium (Gibco, Grand Island, NY, USA) was supplemented with 5 μg/ml insulin (Sigma, St. Louis, MO, U.S.A.), 6 μg/ml transferrin (Boehringer Mannheim, Mannheim, D), 0.35% (w/v) Syperonic F68 (Serva, Heidelberg, FRG) and 1% (w/v) Primatone RL (Sheffield Products, NY, U.S.A.). The medium contained 5.0 g/L glucose and 2.73 g/L sodium bicarbonate. PMS (Phenazine methosulphate, Sigma, St. Louis, MO, U.S.A.) was added at a concentration of $2^* 10^{-6}$ M.

A method developed to correct for the bicarbonate buffer in the culture medium (Bonarius et al., 1995) was applied for the determination of the CO_2 production rate (CER). The CO_2 in the outlet gas was measured by an infrared gas analyzer (Rosemount, Baar, CH). The O_2 uptake rate (OUR) was determined by the mass transfer coefficient $k_1^{02}a$ and the fraction of oxygen in the inlet gas, as described before. Values for $k_1^{02}a$ were determined by the dynamic method (Van 't Riet and Tramper, 1991).

Glucose and lactate were determined with automated enzymatic enzymatic assays (YSI, Yellow Springs, OH), ammonia using an ion-selective electrode, and amino acids by HPLC (Amino Quant 1090, Hewlett-Packard, Paola Alto, CA, USA). Intracellular amino-acid pools were extracted by perchloric acid as described elsewhere (Schmid and Keller, 1992). The cellular composition was measured as described by Xie and Wang (1994): the total lipid fraction was determined by weight after chloroform/methanol extraction, total carbohydrates were analyzed by the phenol-reaction method, total cellular protein was estimated using the Biuret assay, and nucleic acids were quantitated by absorbance at 260 nm after purification according to Chomczynski (1993). Cell size and number were determined using a Casy 1 instrument (Schärfe System, Reutlingen, D) and dry-cell weight was determined after dehydration under vacuum. Antibody titers were measured by a standard ELISA.

Metabolic-flux analysis

A model of the relevant pathways of hybridoma-cell metabolism is shown in Figure 1. Most of the fluxes in this model can be determined by mass-balancing techniques alone. Additional information is reuired for the quentification of fluxes in cyclic pathways. In Figure 1, these fluxes are indicated by solid arrows. It was previously shown that this 'underdetermined' metabolic subnetwork contains three sets of linearly dependent fluxes (Bonarius et al., 1998b):

(i) the malate/pyryvate/oxaloacetate cycle (fluxes 16, 17 and 18),

(ii) glutamine degradation (fluxes 23, 24, and 25), and

(iii) the pentose shunt, glycolsis and TCA cycle (fluxes 1 to 16).

Therefore, three additional constraints are required to determine all fluxes given in Figure 1 by mass-balancing techniques alone:

(i) It was found by ^{13}C-NMR experiments that the flow through pyruvate carboxylase (flux 18) is negligible in hybridoma cells cultured in a hallow-fiber bioreactor (Mancuso et al., 1994). This was recently confirmed for the same hybridoma cell line, the same medium, and the same mode of cultivation as investigated here, by ^{1}H-NMR spectrometry analysis of 3-C-lactate (Bonarius et al., 1998b).

(ii) Although no direct evidence for hybridoma cells exists, it is assumed that the flow through asparagine synthetase (flux 23) is negligible. Street et al. (1993) could not detect labeled asparagine in the medium supernatant of 5-^{15}N-glutamine-fed HeLa and CHO cells, indicating that asparagine synthetase is not active. In cultured mammalian cells, the proposed pathway of glutamine degradation is via glutaminase, rather than via asparagine synthetase (For example: Reitzer et al., 1979, Ardawi and Newsholme, 1984, Mancuso et al., 1994). Only when asparagine becomes limiting, asparagine synthetase may be become active in mammalian cells (Kilberg et al., 1994).

(iii) The flux ratio at the glucose-6-phosphate brachpoint is fitted to the flux distribution measured using isotopic-tracer techniques under the same standard conditions (Bonarius et al., 1998b). The flux through the oxidative branch of the pentose shunt (flux 2) is assumed to be proportional to the biomass synthesis rate.

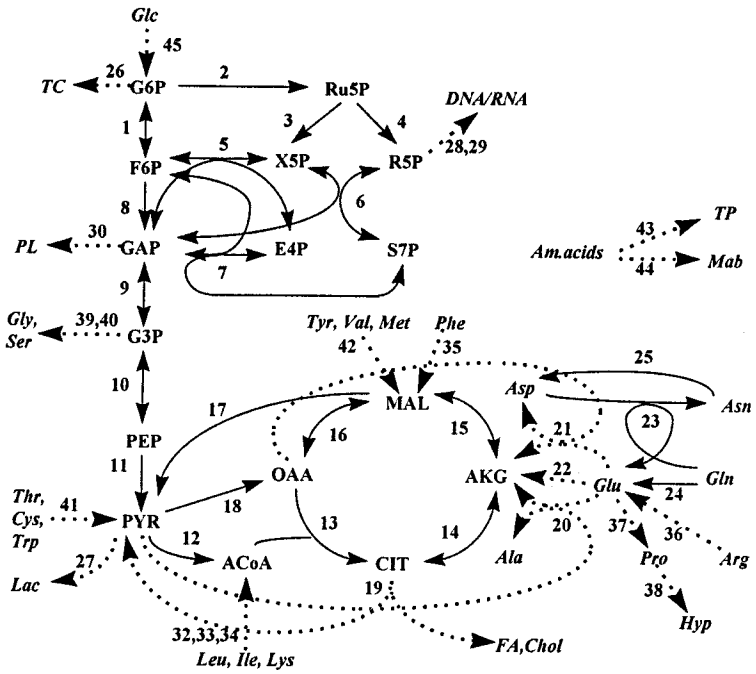

Figure 1. Network of mammalian-cell metabolism. Fluxes that can be quantified by mass balances alone are indicated as dashed lines. To measure the remaining fluxes (solid lines) additional constraints are required.

Results and discussion

Cell density

Hybridoma cells were cultivated in a continuous stirred-tank reactor at different oxygen concentrations. In addition, one experiment was conducted with the artificial electron acceptor PMS in the culture medium. Each time after changing to new culture conditions at least four days of continuous culture were used to dilute metabolites produced during the previous steady state and to allow the viable-cell density to stabilize. Unless stated otherwise, each value presented below is an average of three data points, obtained by daily sampling during three days at steady-state conditions. The viable-cell and viability numbers of the entire experiments are shown elsewhere (Bonarius et al., 1999).

Table I shows the average viable-cell densities, the average glucose and glutamine uptake rates and the average lactate, alanine, ammonia, and monoclonal antibody (Mab) production rates. Only at pO_2 of $\approx$ 0.1%, the culture is oxygen limited and the cell density is significantly lower than cell densities at other oxygen tensions. Similar to data reported by Zupke et al. (1995), at low, albeit non-limiting oxygen tension (pO_2 = 1.0%), the cell density is higher than at higher oxygen tensions. The reason for this is not clear.

PMS, an artifical electron acceptor which diffuses passively through cellular membranes (Hothershall et al., 1979) is toxic for mammalian cells. Sub-lethal concentrations have been found in the order of 10^{-4} M for fibroblasts (Lin et al., 1993) and in the 10^{-6} M range for glioma cells (Mitchel et al., 1989). In order to determine an affective but sub-lethal PMS concentrations for hybridoma cells, T-flask experiments were conducted. Figure 2. shows that PMS is toxic above $5^* 10^{-6}$ M for hybridoma cells. Continuous-culure experiments are therefore conducted at a concentration of $2^* 10^{-6}$ M PMS. In table I it is shown that the viable cell density is slightly lower at this concentration during this steady state ($1.30^* 10^6$ vs $1.46^* 10^6$ cells/ml, respectively).

Metabolic production and consumption rates

The extracellular production and consumption rates of amino acids, glucose, ammonia, lactate, oxygen, carbon dioxide and monoclonal antibody were determined. Also, the intracellular concentrations of amino acids, lactate, total cell protein, DNA, RNA, and the total lipid and carbohydrate contents were measured.

Table 1. Average viable-cell density (10^6 cells/ml) and average uptake and production rates of indicated metabolites (10^{-12} mol.cell^{-1}.day^{-1}) under different conditions. Values between parentheses indicate standard deviations

	0.1% pO_2	0.1% pO_2	30% pO_2	50% pO_2	100% pO_2	30% pO_2 and $2^* 10^{-6}$ M PMS
Viable cell density	1.16 (0.14)	1.78 (0.05)	1.46 (0.03)	1.58 (0.06)	1.47 (0.08)	1.30 (0.10)
Glucose uptake	12.3 (0.13)	7.27 (0.43)	6.34 (0.35)	5.37 (0.22)	5.82 (0.17)	4.02 (0.61)
Lactate production	19.1 (1.61)	10.7 (0.82)	7.48 (0.64)	5.27 (0.67)	7.03 (0.45)	3.43 (0.21)
$Y_{LAC/GLC}$	1.56	1.48	1.18	0.98	1.21	0.86
Glutamine uptake	2.02 (0.20)	1.40 (0.05)	1.52 (0.05)	1.62 (0.21)	1.90 (0.08)	1.03 (0.15)
Alanine production	1.15 (0.06)	0.77 (0.02)	1.23 (0.04)	0.98 (0.15)	1.23 (0.04)	1.36 (0.01)
Ammonia production	0.88 (0.13)	0.75 (0.05)	1.22 (0.11)	0.72 (0.14)	1.07 (0.12)	1.42 (0.09)
Specific Mab production (pg. cell^{-1}. day^{-1})	14.3 (1.25)	13.5 (0.59)	17.0 (0.49)	13.8 (0.61)	14.2 (0.13)	21.7 (2.05)

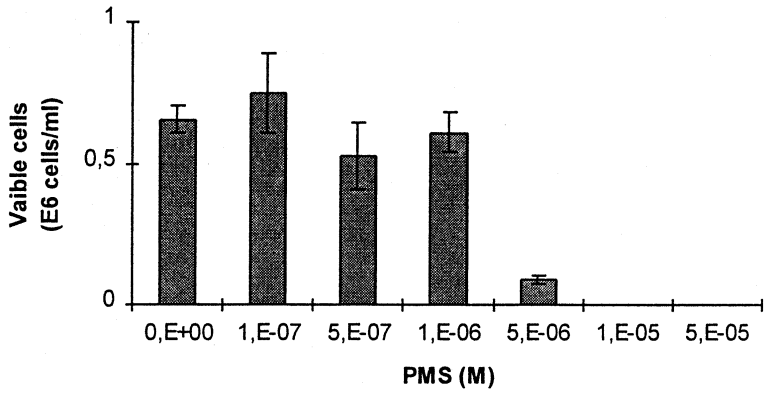

Figure 2. Viable-cell densities at different concentrations of PMS after two days of cultivation. Averages for two T-flask experiments are shown.

Only a limited amount of the measured data are shown here in Tables 1–3 and in Figures 3–5. Complete tables with raw data are published in elsewhere (Bonarius et al., 1999), where it is demonstrated that the carbon and nitrogen balance over all metabolic rates are closed.

Glucose concumption and lactate production

It has been established that the specific glucose consumption and lactate production increase at low pO_2 levels (below ca. 10% of air saturation) (Miller et al., 1987; Ozturk and Palsson, 1990; Zupke et al., 1995). The data shown in Table 1 and Figure 3a are in agreement with these observations. In particular at oxygen-limiting conditions ($pO_2 \approx 0.1\%$) the glucose uptake and lactate production rate increase strikingly, as animal cells change from 'complete' oxidation of glucose to CO_2 to anaerobic glycolysis. The addition of PMS has an opposite effect on glucose metabolism: the glucose decreases. In addition, the lactate yield per glucose decreases due to the attificial electron acceptor (Table 1), which is the consequence of competition between lactate dehydrogenase and PMS for NADH. Together, these two effects cause a decrease in the specific lactate production rate of more than 50% compared to the control culture (pO_2 = 30%). This suggests that addition of PMS can be used to decrease lactate formation in mammalian-cell culture without affecting cell density, which may become sigmificant for high-cell density cultures, where lactate inhibition constraints further cell growth. An additional beneficial effect of PMS is the increase in specific

Table 2. Fluxes values of selected reactions estimated based on metabolite balances and the assumption that the pentose shunt the pentose shunt is linearly dependent on the biomass-synthesis rate. Values are in 10^{12} mol.cell^{-1}.day^{-1}

Condition	0.1% pO_2	1.0% pO_2	30% pO_2	50% pO_2	100% pO_2	30% pO_2 and 10^{-6} M PMS
Oxidative branch pentose shunt (x_2	1.44	1.63	1.76	1.81	1.65	2.10
Glycoclysis (x_8	21.2	12.6	10.6	8.59	9.58	5.85
Pyruvate dehydrogenase (x_{12}	0.10	0.76	1.54	1.90	1.12	2.19
Isocitrate dehydrogenase	1.08	1.43	2.85	2.94	2.29	2.20
α-Ketoglutarate dehydrogenase (x_{15}	2.45	0.17	1.37	1.54	0.85	3.12
Malic enzyme (x_{17}	–0.76	–0.04	0.06	0.05	0.10	0.30
Glutamate dehydrogenase (x^a_{22}	–0.53	–0.31	–0.11	–0.17	–0.11	0.03
Lactate dehydrogenase (x^a_{27}	19.1	10.7	7.48	5.27	7.03	3.43

[a] The values of the glutamate-dehydrogenase and the lactate-hydrogenase flux is not influenced by this assumption, as it can determined by strictly using metabolite balances (See also Figure 1).

monoclonal-antibody production. Table 1 shows that the Mab production increase 27% compared to the control culture.

In contrast to normal proliferating cells, which regulate glycolysis dependent on the requirement for ATP according to the Pasteur effect (Eigenbrodt et al., 1985), the glycolysis activity of tumor cells in insensitive to high concentrations of oxygen (Caroll et al., 1978). In Figure 3a it is shown that this also accounts for hybridoma cells.

Oxidative degradation of amino acids

In mammalian-cell metabolism, a number of amino acids are not only used as building blocks for biomass, but also as fuel (Stryer, 1988). Other amino acids, such as glycine, proline, or alanine are produced by most continuous mammalian cell lines (Lanks and Li, 1988). Fluxes of amino-acid degradation and production pathways are determinable by mass-balancing techniques (Xie and Wang, 1996; Bonarius et al., 1996; Vriezen and Van Dijken, 1998; Follstad et al., 1999). Flux analysis of amino-acid metabolism is therefore an appropriate tool to test the hypothesis that under hypxic conditions, when the $NAD(P)^+$/NAD(P)H-ratio is low (Zupke et al., 1995), steady state fluxes by which NAD(P)H are produced decrease. At high pO_2 levels or during PMS-stress, the opposite may occur; steady state fluxes of reactions in which NAD(P)H is produced increase as a result of increased $NAD(D)^+$.NAD(P)H ratio. The 'net-catabolic rate of amino acid A' ($r_{nc,A}$) (Bonarius et al., 1996) is a measure for the conversion rate of amino acids corrected for biosynthesis requirements, and is used here to test this hypothesis. The $r_{nc,A}$ is determined from the concumption rate, the biomass synthesis rate (including Mab synthesis) and the fraction of each amino acid in biomass. A negative value for $r_{nc,A}$ indicates that A is degraded, while a positive value indicates that A is produced.

In Table 3 the net catabolic rates of amino acids are shown for 6 different culture conditions It appears that arginine, leucine, lysine, isoleucine, methionine, and cysteine are degraded at relatively high rates $\sim 10^{-13}$ mol.cell^{-1}.day^{-1}). The net stoichiometric equations of the oxidative degradation of these amino acids are given in Table 4. During oxidation of arginine, (iso)leucine and methionine, $NAD(P)^+$ is reduced to NAD(P)H. This is not case for degradation of cysteine. Figure 4a shows the average values of the measured degradation rates of these amino acids, together with their standard deviations. At oxygen limitation ('0') and low pO_2 ('1') the steady state flux at which leucine, lysine, and isoleucine are catabolized are significantly lower than under standard conditions (30% or 50% of air saturation). When the artificial electron acceptor PMS is added to the culture medium, the fluxes increase, which is particularly the case for lysine and arginine degradation. Methionine and arginine degradation increase slightly at higher pO_2 levels, but the differences are not as significant as for (iso)leucine. This may be a consequence of the fact that more oxidative power, that is more moles of NAD^+ per mole amino acid, is required for the degradation of (iso)leucine and lysine than for the degradation of methionine and arginine (See also Table 4). In contrast to (iso)leucine, lysine, arginine and methionine, the degradation of cysteine does not require

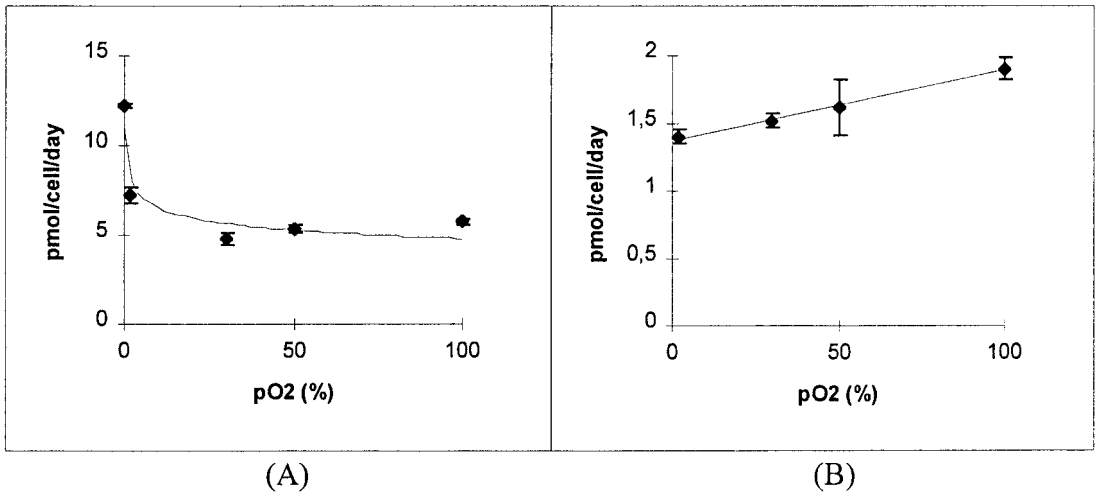

Figure 3. Specific glucose (A) and glutamine (B) uptake rate (pmol. cell^{-1}. day^{-1}) of continuously cultured hybridoma cells as a function of oxygen tension (% of air saturation). At oxygen limitation ($pO_2 \approx 0.1\%$) the glutamine uptake increases to 2.02 pmol/cell/day (not shown in Figure B).

Table 3. Net catabolic rates of amino acids of continuous-cultured hybridoma cells at different dissolved oxygen concentration. pO_2 in % of air saturation, net catabolic rates in mol.cell^{-1}.day^{-1}. PMS indicates steady state with Phenazine Methosulfate ($2^{*}10^{-6}$ M) in the culture medium. A negative value indicates that the amino acid is degraded. Amino acids are given in order of chromatographic separation

PO_2	0.1%	1%	30%	50%	100%	PMS
ASP	2,04E-13	1,65E-13	6,80E-14	1,65E-13	1,35E-13	2,07E-13
GLU	1,97E-13	1,54E-13	3,23E-14	1,94E-13	1,83E-13	2,16E-13
ASN	3,93E-14	3,06E-14	1,09E-13	2,61E-14	4,01E-14	1,33E-14
SER	8,29E-14	8,66E-14	2,08E-13	1,97E-13	2,26E-13	3,39E-13
GLN	–1,80E-12	–1195E-12	–1,28E-12	–1,39E-12	–1,69E-12	–1,85E-12
HIS	–2,73E-14	–1,79E-14	–2,05E-14	–2,59E-14	–3,82E-14	–2,23E-14
GLY	1,16E-13	1,23E-13	1,38E-13	1,41E-13	1,23E-13	1,49E-13
THR	–2,96E-14	–4,46E-14	–3,17E-14	–4,12E-14	–1,15E-14	–2,22E-14
ALA	1,41E-12	1,07E-12	1,56E-12	1,30E-12	1,40E-12	1,73E-12
ARG	–2,64E-14	–1,87E-14	–8,46E-14	–2,37E-14	–4,67E-14	–1,17E-13
TYR	–2,90E-14	–1,96E-14	–2,39E-14	–2,04E-14	–3,16E-14	–3,14E-14
CYS	–1,10E-13	–6,43E-14	–7,16E-14	–6,17E-14	–7,30E-14	–8,55E-14
VAL	3,13E-14	3,12E-14	–4,20E-15	5,42E-15	–3,50E-14	–1,17E-14
MET	–6,71E-14	–5,45E-14	–6,35E-14	–6,44E-14	–7,79E-14	–9,36E-14
TRP	5,86E-16	–3,29E-15	–1,10E-14	–3,13E-15	6,84E-15	–1,86E-14
PHE	–6,08E-15	1,17E-16	3,48E-15	7,08E-16	–4,24E-15	–2,49E-14
ILE	–1,18E-13	–1,19E-13	–2,62E-13	–2,00E-13	–2,10E-13	–2,99E-13
LEU	–1,79E-13	–1,81E-13	–4,08E-13	–3,17E-13	–3,56E-13	–4,83E-13
PYS	–5,28E-14	–5,23E-14	–9,30E-14	–7,04E-14	–1,04E-13	–1,27E-13
PRO	3,41E-13	3,20E-13	2,34E-13	2,83E-13	2,80E-13	6,71E-14
HYP	3,04E-13	2,12E-13	2,53E-13	2,44E-13	2,54E-13	3,45E-13

Table 4. Net stoichiometric equations of amino acid metabolism (Only the reactions of amino acids that are discussed in the text are shown)

Amino acids that are degraded in hybridoma cells	
Arginine	ARG + $2H_2O$ + AKG + → 2GLU + Urea + NADH
Lysine	LYS + H_2O + $3NAD^+$ + 2FAD + 2AKG →
	ACoA + NH_3 + $2FADH_2$ + 3NADH + 2GLU + CO_2
Leuzine	LEU + AKG + $2H_2O$ + ATP + CoASH + NAD^+ + FAD →
	GLU + ADP + POH + ACoA + NADH + FADH + AAA
Isoleucine	ILE + AKG + $2H_2O$ + ATP + 2CoASH + $2NAD^+$ + FAD →
	GLU + SuCoA + ADP + POH + ACoA + 2 NADH + FADH
Methionine	MET + SER + CoASH + H_2O + NAD^+ + ATP + THF →
	CYS + SuCoA + methylene-THF + NH_3 + NADH + ADP + POH
Cysteine	CYS + AKG → GLU + S + PYR
Amino acids that are produced by hybridoma cells	
Proline	GLU + ATP + 2NADPH → PRO + H_2O + ADP + POH + $2NADP^+$
Glycine	SER + THF → GLY + methyl-THF + H_2O
Serine	GLU + H_2O + 3PG + NAD^+ → SER + AKG + POH + NADH

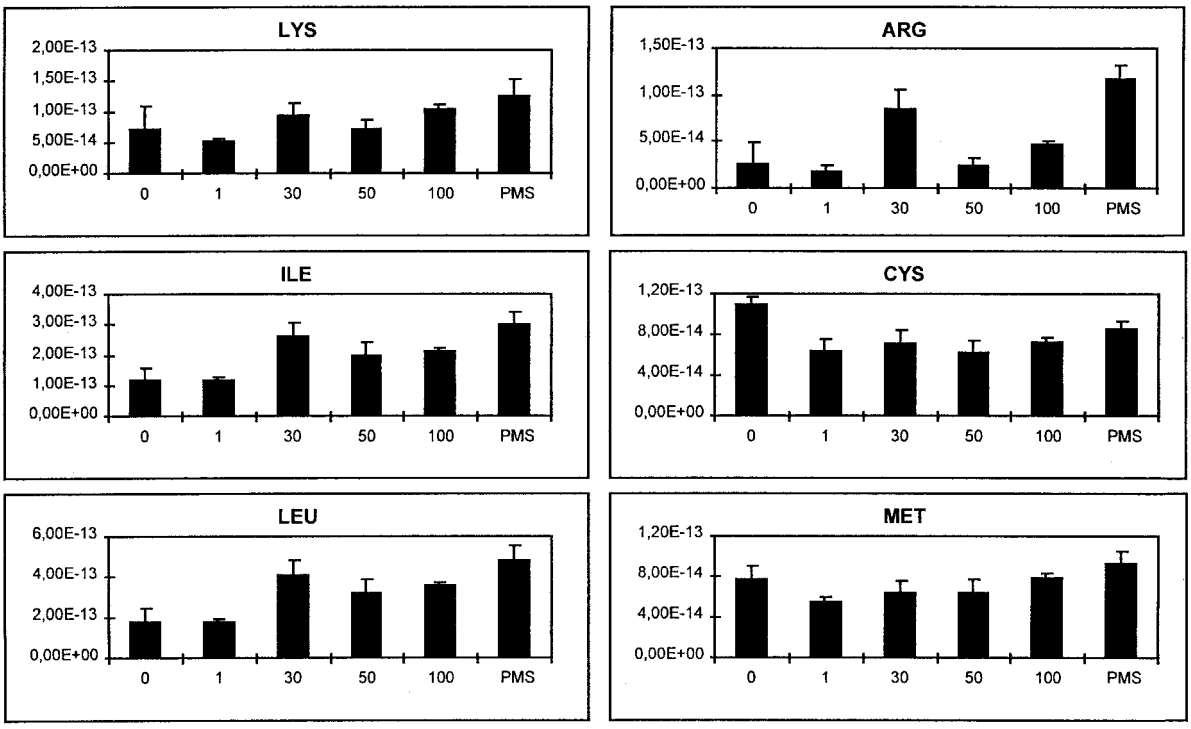

Figure 4a. Degradation rates of lysine, isoleucine, leucine, arginine, cysteine, and methionine for 6 different steady states. Values are shown as absolute values of net catabolic rates, given in mol. $cell^{-1}$. day^{-1}, and are averages from 3 data points during each steady states. Standard deviations are shown as T-bars.

NAD^+. Figure 4a shows that the cysteine degradation rate does not increase at higher pO_2 and only slightly under PMS-stress.

Biosynthesis of proline, glycine, and serine

The 'net catabolic rates' of proline, glycine, and serine are non-negative (Table 3), which indicates that these metabolites are produced from other amino acids in hybridoma cells. Figure 4b shows the average values of the measured production rates of these amino acids together with their standard deviations for 6 steady states. The serine production, which is dependent on the availability of NAD^+, is relatively low under oxygen limitation and low pO_2, which is consistent with the low NAD^+/NADH ratios under these conditions (Zupke and co-workers (1995)). It appears that the steady state proline-synthesis flux is independent of pO_2. This may be explained by the fact that in the proline synthesis pathway no NAD^+/NADH is co-metabolized. Instead, proline synthesis requires two moles of NADPH per one mole produced proline. When hybridoma cells are grown in medium supplemented with PMS, which oxidizes NADPH, the proline production decreases more than 3-fold.

Glutamate dehydrogenase

Glutamate dehydrogenase (flux 22) catalyses the following oxidative deamination reaction:

$$\begin{gathered}\text{glutamate} + NAD^+ + H_2O \leftrightarrow \\ (\text{or } NADP^+) \\ \alpha\text{-ketoglutarate} + NH_4^+ + NADH + H^+ \\ (\text{or NADPH})\end{gathered}$$

In contrast to fluxes in linearly dependent subnetworks, which require additional contraints for their quantification, flux 22 can be determined on the basis of mass-balance equations alone. Its value is therefore not influenced by any of the constraints A, B, or C mentioned in the Materials and Methods Section. Recently, we showed that glutamate dehydrogenase is activated in the direction of α-keteglutarate to glutamate in ammonia-stressed hybridoma cells (Bonarius et al., 1998a). Here it is shown that, in agreement with data reported by Zupke et al. (1995), also at lower oxygen tensions the glutamate-dehydrogenase flux reverses into the glutamte-producing direction (Table 2). The opposite is the case in PMS-stressed hybridoma cells: the glutamate-dehydrogenase flux increases towards the direction of α-ketoglutarate and NAD(P)H.

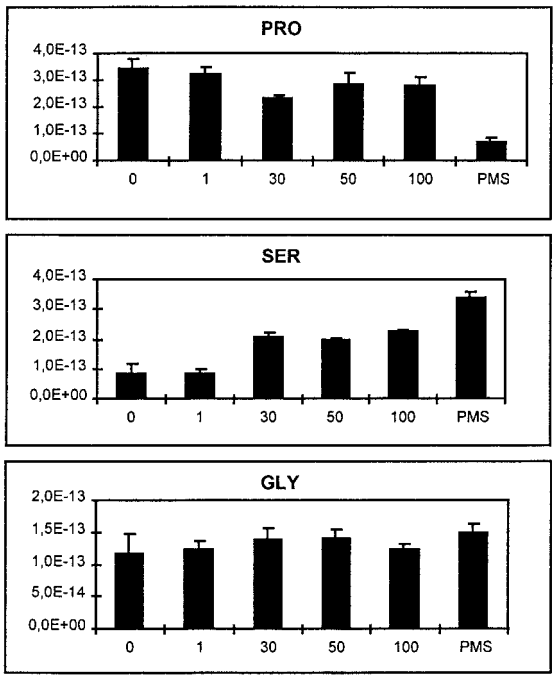

Figure 4b. Net production rates of proline, serine, and glycine for 6 different steady states. Values are given as in mol.cell^{-1}.day^{-1} and are averages from 3 data points during each steady states. Standard deviations are shown as T-bars.

This is in agreement with the fact that by the action of PMS NAD(P)H-producing fluxes such as the pentose- and malate-shunt flux (Greenbaum et al., 1971), the serine synthesis flux (Figure 4b) and the (iso)leucine degradation flux (Figure 4a), increase.

Glutaminolysis and pyruvate oxidation

Similar to data reported by Miller et al. (1987) and Jan et al. (1997), the glutamine uptake decreases at lower levels (Figure 3b), probably because there is not sufficient oxygen available for complete glutamine oxidation. At oxygen-limiting conditions ($pO_2 \approx 0.1\%$) however, the glutamine uptake increases (Table 1). This may be explained by the fact that oxygen-limited hybridoma cells have to rely on glutaminolysis for energy production. Hornsby and Gill (1981) showed that when cells suffer a block in puryvate oxidation, which was selectively achieved by cortisol treatment, the glutaminolysis activity increased (Eigenbrodt et al., 1985). This is in agreement with flux data shown in Table 2, and with flux data reported by Zupke et al. (1995). Both these results show that the pyruvate dehydrogenase is significantly smaller during oxy-

gen limitation. Investigations with adrenocortical cells showed that the decrease in puruvate oxidation and the simultaneous increase in glutamine respiration is not only associated with inhibition of pyruvate dehydrogenase, but also with a lower isocitrate-dehydrogenase flux (Hornsby and Gill, 1981). The same trend is found here for oxygen-limited hybridoma cells (Table 2). Other support for the low pyruvate- and isocitrate-dehydrogenase activity at low oxygen tension comes from the analysis of intracellular isocitrate and pyruvate pools, which were found to be significantly lower at low pO_2 (Zupke et al., 1995).

Pentose-phosphate pathway and malate shunt

Isotopic-tracer experiments with 1-^{14}C-glucose and 6-^{14}C-glucose have shown that both the pentose-shunt (x_2) and the malate-shunt (x_{17}) flux increase significantly when mammalian cells are incubated with the artificial electron acceptor PMS (Greenbaum et al., 1971, Hothershall et al., 1979. Lin et al., 1993). Here, the flux through these metabolic shunts is estimated by extracellular uptake and consumption rate and mass-balance equations, in combination with the assumption that the pentose-shunt flux is linearly dependent on the biomass synthesis rate. The flux values for the malic shunt and in particular the pentose shunt are high compared to the other culture conditions (Table 2). This suggests that the well-established effect of PMS is qualitatively measurable using mass-balancing techniques, even if the set of mass-balance equations is underdetermined. For quantitative data of fluxes in cyclic pathways however, isotopic-tracer experiments remain indispensable.

Conclusions

– The (steady-state) degradation rates of lysine, leucine, isoleucine, methionine, and arginine of hybridoma cells increase at higher pO_2 levels and under PMS stress.
– The proline synthesis flux decreases 3-fold in PMS-containing medium, and the serine production rate increases under oxidative stress.
– Sub-lethal levels of the artificial electron acceptor PMS give 50% lower lactate-production rates and 27% higher Mab-production rates compared to the control in hybridoma-cell culture.
– Under oxidative stress, the glutamate-dehydrogenase flux into the direction of α-ketoglutarate and NH_4^+ increases. In contrast, under oxygen-limiting conditions the glutamate-dehydrogenase flux reverses into the direction of glutamate.
– It can be shown by flux-balancing techniques that the artificial electron acceptor PMS causes an increase of the pentose- and malate-shunt flux relative to control cultures.

References

Ardawi MSM & Newsholme EA (1984) Glutamine metabolism in lymphoid tissues. In: Häussinger D & Sies H (eds.), Glutamine Metabolism in Mammalian Tissues. (pp. 235–246) Springer-Verlag, Berlin.

Bonarius HPJ, de Gooijer CD, Tramper J & Schmid G (1995) Determination of the respiration quotient in mammalian cell culture in bicarbonate-buffered media. Biotechnol Bioeng 45: 524–535.

Bonarius HPJ, Hatzimanikatis V, Meesters KPH, de Gooijer CD, Schmid G & Tramper J (1996) Metabolic flux analysis of hybridoma cells in different culture media using mass balances. Biotechnol Bioeng 50: 299–318.

Bonarius HPJ, Schmid G & Tramper J (1997) Flux analysis in undetermined metabolic networks: The quest for the missing constraint. Trends in Biotechnol 15: 308–314.

Bonarius HPJ, Houtman JHM, de Gooijer CD, Tramper J & Schmid G (1998a) The activity of glutamate dehydrogenase is increased in ammonia-stressed hybridoma cells. Biotechnol Bioeng 57: 447–453.

Bonarius HPJ, Timmerarends B, de Gooijer CD & Tramper J (1998b) Metabolite balancing techniques versus ^{13}C tracer experiments to determine metabolic fluxes in hybridoma cell. Biotechnol Bioeng 58: 258–262.

Bonarius HPJ, Houtman JHM, Schmid G, de Gooijer CD & Tramper J (1999) Error analysis of metabolic-rate measurements in mammalian-cell culture by carbon and nitrogen balances. Cytotechnol 29: 167–175.

Caroll RC, Ash JF, Vogt PK & Singer SJ (1978) Reversion of transformed glycolysis to normal by inhibition of protein synthesis in rat liver kidney cells infected with temperature-sensitive mutant of Rous sarcoma virus. Proc Natl Acad Sci USA 75: 5015–5021.

Chomczynski P (1993) A reagent for the single-step simultaneous isolation of ma, dna and proteins from cell and tissue samples. Biotechniques 15: 532.

Eigenbrodt E, Fister P & Reinacher M (1985) New perspectives on carbohydrate metabolism in tumor cells. In: Breitner R (ed.), Regulation of Carbohydrate Metabolism. Vol. 2 (pp. 141–169) CRC Press, Boca Raton.

Fell DA & Small JA (1986) Fat synthesis in adipose tissue. An examination of stoichiometric constraints. Biochem J 238: 781–786.

Ferrance JP, Goel, A & Ataai MM (1993) Utilization of glucose and amino acids in insect sultures: quantifying the metabolic flows within primary pathways and medium development, Biotechnol Bioeng 42: 697–707.

Follstad BD, Balcarcel RR, Stephanopoulos G & Wang DIC (1999) Metabolic flux analysis of hybridoma continuous culture steady state multiplicity. Biotechnol Bioeng 63: 675–683.

Greenbaum AL, Gumaa KA & McLean P (1971) The distribution of hepatic metabolites and the control of pathways of carbohydrate metabolism in animals of different dietary and hormonal status. Arch Biochem Biophys 143: 617–663.

Hornsby PJ & Gill GN (1981) Regulation of glutamine and pyruvate oxidation in cultured adrenocortical cells by cortisol, antioxidants, and oxygen: effects on cell proliferation. J Cell Physiol 109: 111–123.

Hothershall JS, Baquer NA, Greenbaum AL & McLean P (1979) Alternative pathways of glucose utilization in brian. Changes in the pattern of glucose utilization in brain during development and the effect of phenazine methosulfate on the integration of metabolic routes. Arch Biochem Biophys 198: 478–492.

Jan DHC, Petch DA, Huzel N & Butler M (1997) The effect of dissolved oxygen concentration on the metabolic profile of murine hybridoma grown in serum-free medium in continuous culture. Biotechnol Bioeng 54: 153–164.

Kilberg MS, Hutson RG & Laine RO (1994) Amino acid-regulated gene-expression in eukaryotic cells. FASEB J 8: 13–19.

Mitchell SL, Ross BD, Krick T & Garwood M (1989) Gas chromatographic-mass spectrometric analysis of hexose monophosphate shunt activity in cultured cells. Biochem Biophys Res Comm 158: 474–479.

Nyberg GB, Balcarcel RR, Follstad BD, Stephanopoulos G & Wang DIC (1999) Metabolism of peptide amino acids by Chinese hamster ovary cells grown in a complex medium. Biotechnol Bioeng 62: 324–335.

Lanks KW & Li PW (1988) End products of glucose and glutamine metabolism by cultured cell lines. J Cell Phys 135: 151–155.

Lin YY, Cheng WB & Wright CE (1993) Glucose metabolism in mammalian cells as determined by mass isotopomer analysis. Anal Biochem 209: 267–273.

Mancuso A, Sharfstein ST, Tucker SN, Clark DS & Blanch HW (1994) Examination of primary metabolic pathways in a murine hybridoma with carbon-13 nuclear magnetic resonance spectroscopy. Biotechnol Bioeng 44: 563–585.

Miller WM, Wilke CR & Blanch HW (1987) Effects of dissolved oxygen concentration on hybridoma growth and metabolism in continuous culture. J Cell Phys 132: 524–530.

Ozturk SS & Palsson BO (1990) Effects of dissolved oxygen on cell growth, metabolism, and antibody production kinetics in continuous culture. Biotechnol Progr 6: 121–128.

Reitzer LJ, Wice BM & Kennel D (1979) Evidence that glutamine, not sugar, is the major energy source for cultured HeLa cells. J Biol Chem 254: 2669–2676.

Savinell JM & Palsson BO (1992) Network analysis of intermediary metabolism using linear optimization. J Theor Biol 154: 421–454.

Schmid G & Keller T (1992) Monitoring hybridoma metabolism in continuous suspension culture at the intracellular level. Cytotechnol 9: 217–229.

Sharfstein ST, Tucker SN, Mancuso A, Blanch HW & Clark DS (1994) Quantitative in vivo nuclear magnetic resonance studies of hybridoma metabolism. Biotechnol Bioeng 43: 1059–1074.

Street JC, Delort AM, Braddock PS & Brindle KM (1993) A $^{1}H/^{15}N$ NMR study of nitrogen metabolism in cultured mammalian cells. Biochem J 291: 301–304.

Stryer L (1988) Biochemistry, 3rd edition. WH Freeman and Company, New York.

Vallino JJ & Stephanopoulos G (1989) Flux determination in cellular bioreaction networks: application to lysine fermentations. In: Sikdar SK, Bier M & Todd P (eds.), Frontiers in Bioprocessing (pp. 205–219) CRC Press, Boca Raton, FL.

Van 't Riet K & Tramper J (1991) Basic bioreactor design. Marcel Dekker, New York.

Varma A & Palson BO (1994) Metabolic flux balancing: Basic concepts, scientific and practical use. Biol Technology 12: 994–998.

Vriezen N & van Dijken JP (1998) Fluxes and enzyme activities in central metabolism of myeloma cells grown in chemostat culture. Biotechnol Bioeng 59: 28–39.

Xie L & Wang DLC (1994) Stoichiometric analysis of animal cell growth and its application in medium design. Biotechnol Bioeng 43: 1164–1174.

Xie L & Wang DIC (1996) Material balance studies on animal-cell metabolism using a stoichiometrically based reaction network. Biotechnol Bioeng 52: 579–590.

Zupke C, Sinskey AJ & Stephanopoulos G (1995) Intracellular flux analysis applied to the effect of dissolved-oxygen on hybridomas. Appl Microbiol Biotechnol 44: 27–36.